Proceedings of the Estonian Academy of Sciences,
2022, **71**, 4, 350–360
https://doi.org/10.3176/proc.2022.4.05
Available online at www.eap.ee/proceedings

LASER WELDING OF PLASTICS

Laser beam positioning in quasi-simultaneous laser transmission welding of polymers

Simonas Mindaugas Jankus* and Regita Bendikienė

Department of Production Engineering, Faculty of Mechanical Engineering and Design, Kaunas University of Technology, Studentų g. 56, LT-51424 Kaunas, Lithuania

Received 1 April 2022, accepted 6 September 2022, available online 15 November 2022

Abstract. The main objective of this study was to investigate the influence of laser beam positioning on the quality of the polymer joint weld. The laser scan path from the centre of the weld was varied, and its effect on the joint performance was evaluated. Three laser transparent-absorbent polymer pairs with different transmissions were subjected to the following tests: burst pressure, thermal shock, and leakage tests. The tests were performed to evaluate the strength and tightness of the weld. The strongest joints, with an average burst pressure value of 6.4 bar, were obtained by positioning the laser beam at a shift of 0.0 mm, and the lowest joint strength of 5.8 bar at a shift of 0.7 mm. The shift of the laser beam from the centre of the weld affected the heterogeneous melting of the polymers, which increased the heating time required to reach the targeted meltdown: 4.2 s was reached at a 0.0 mm shift and up to 10 s at a 0.7 mm shift. This led to joint overheating, forming of pores, and decreased weld strength. The polymer pair with modulated laser radiation transmission and an absorbent part showed inhomogeneous energy deposition across the weld seam and the formation of the heat-affected zone (HAZ) during quasi-simultaneous welding. The quality of this pair was improved using a 0.0 mm shift and laser power from 330 W to 350 W. As a result, no weld leakage was detected after 50, 75, and 100 thermal shock cycles.

Keywords: polymer welding, laser beam positioning, joint strength, pores, modulated transmission, laser power.

1. INTRODUCTION

Laser transmission welding (LTW) technology is widely used in the automotive, medical, electronic device industries, and for joining complex polymer assemblies. LTW offers unique advantages in weld quality and mechanical properties compared to conventional polymer welding processes [1–6].

LTW performance depends on material properties, process parameters, laser irradiation, and application strategies. Various laser irradiation strategies have been developed and implemented in laser welding, varying in laser scanning techniques, cycle times, and process flexibility. Welding is influenced by the laser irradiation methods that define the process capabilities, including weld profile, part size, part variety, and cycle time. The four main variations of LTW are contour, simultaneous, quasi-simultaneous, and mask welding techniques [2–4]. In the contour LTW technique, the laser beam moves along the predefined weld path to form the weld, being the simplest LTW variant. In simultaneous laser welding, the joint is achieved using a precise arrangement of laser diode modules that simultaneously irradiate the entire weld contour. The joint configuration can be welded using special beam-shaping diffractive optical elements (DOE), avoiding the complex arrangement of laser modules along the laser weld contour. In the quasi-simultaneous laser welding (QSLW) technique, the laser beam passes through the parts to be welded several times at very high speed. By using the galvo mirror system, the laser beam is directed according

* Corresponding author, simonas.jankus@ktu.edu

to a predetermined weld contour. Nowadays, quasi-simultaneous laser welding is often used in batch production, especially for welding 2D contours. In mask welding, a mask is placed between the laser optics and the material to be welded so that the laser beam only hits the uncovered surface. Radial welding can be performed using contour, quasi-simultaneous or simultaneous irradiation methods [3].

Extensions of LTW irradiation strategies include, for example, transmission laser welding using incremental scanning technique process, which is performed by overlapping the circular movement of the laser beam along the weld contour. The weld width can be varied for the same weld contour, for example, by changing the circle's diameter [3,6,7]. The TWINQUASI welding process technique is a modified quasi-simultaneous welding technique using two lasers and optical scanners. This method allows for doubling the scan length in the same welding period while maintaining the same scan frequency as QSLW. It also produces 1000 mm long seams in a short welding time of 2.6 s [3,8]. A new QSLW scanning strategy was also introduced where the laser beam path was offset to a different location for each laser beam pass. The QSLW beam offset scanning technique enables to produce wider welds [9]. Recent studies have used various scanning patterns and evaluated temperature fields in the polymeric joints. Different scanning structures were applied to optimize the temperature distribution across the weld. The performance of various QSLW scanning patterns was experimentally assessed [10–12].

The joining of polymers by positioning the laser beam at a shift relative to the centre of the weld seam during quasi-simultaneous laser transmission welding has not been well studied. This study aims to determine the relationship between the laser beam's scan path shift from the centre of the weld and the joint structure, strength, and weld cycle time. The idea is to obtain practical results using different laser transparent polymers that would be valuable in the industry.

2. MATERIALS AND METHODS

2.1. Materials

A semi-crystalline structure, glass fibre reinforced polyphthalamide (PPAGF40) polymer pairs with three different transmissions for laser radiation (transparent part) and laser absorbent parts were used. The two pairs had uniform laser transmissions of 20% and 30%. This means that 20% or 30% of laser radiation along the perimeter of the weld passed through the transparent polymer before reaching the absorbent polymer. The third pair had modulated transmission through the transparent part from 27% to 47%. Modulated transmission means that the perimeter of the transparent polymer is inhomogeneous, with some areas transmitting 27% of the laser radiation and others as much as 47%. Each laser transparent-absorbent polymer pair was further indexed in the text by laser beam transmission through the transparent polymer: I-30 pair with 30% transmission, II-20 with 20%, and III-m with modulated transmission ranging from 27% to 47%. A dimensional view of the polymer joint assembly is shown in Fig. 1. The weld width of the laser absorbing polymer sample was 1.5 mm, and the thickness of the transparent laser polymer was 1.6 mm. The weld perimeter as the distance travelled by the laser beam between each scan was 340 mm (total length of the 2D weld contour). The dimensions of the laser transparent-absorbent polymer assembly were 125 × 67 × 33 mm. All welded specimens of PPAGF40 polymer had closed geometrical contours. The laser assembly was designed with flash traps that shut off the weld flash when it reached a specifically targeted meltdown.

Table 1. Characteristics of polyphthalamide PPAGF40

Main characteristics	PPAGF40
Polymer structure	semi-crystalline
Transmittance of transparent polymer	20%, 30% and 27–47%
Glass fibre (GF)	40 wt.%
Melting point	315–325 °C
Density	1.50–1.53 g/cm^3
Additives in polymer	Carbon black (CB)

The main mechanical and physical characteristics of the polymer PPAGF40 are presented in Table 1.

2.2. Quasi-simultaneous laser transmission welding

The beam's diameter did not change with respect to the x-y welding plane and remained constant during welding for all polymer assemblies. The welding system consisted of the following components: a diode laser source, an optical fibre for transmitting laser radiation, a galvanometric scanner, focusing optics, a pneumatic clamping system with appropriate fixing elements for setting the position of polymers to be welded, and a meltdown measurement system. The laser beam was directed along the closed-loop 2D weld contour by a galvo mirror system (Fig. 2).

In this research, the shift of the laser beam on the polymer assembly was selected by positioning the laser beam at a shift in relation to the centre of the weld seam. The shift of the laser beam from the centre of the weld was varied by changing the defined coordinates of the weld contour. The basic characteristics of the laser welding systems used in this study are presented in Table 2.

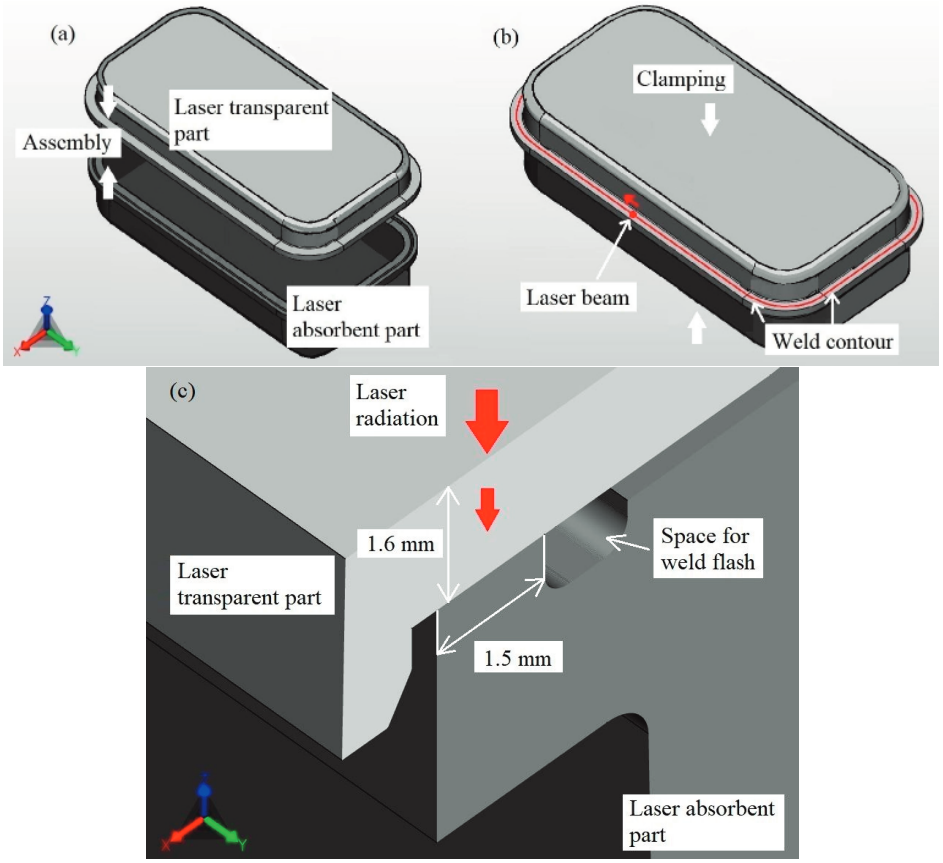

Fig. 1. General view of a polymer pair: (a) laser transparent-absorbent polymer assembly; (b) welding process scheme; (c) cross-sectional view of a polymer pair with dimensions.

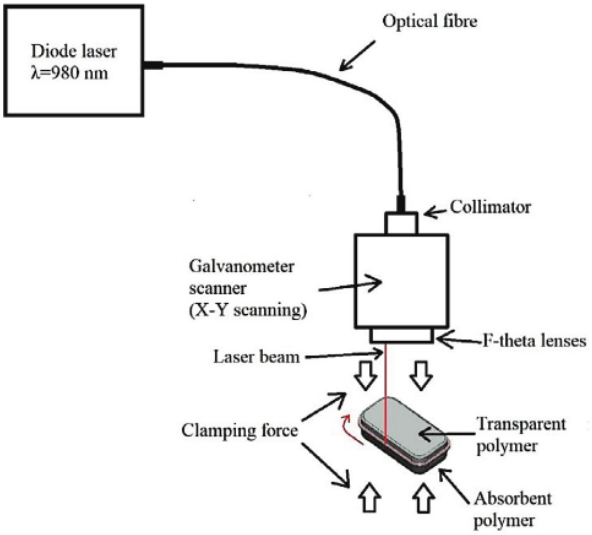

Fig. 2. Schematic diagram of the setup for the quasi-simultaneous laser transmission welding experiment.

Table 2. Characteristics of the laser welding system

Characteristics	Description
Type of laser	Fibre-coupled diode laser
Welding technique	Quasi-simultaneous laser welding
Wavelength	980 nm
Operation mode	Continuous wave mode (CW)
Laser beam diameter	3 mm
Laser intensity distribution	Gaussian distribution

In this study, the value of the targeted meltdown (weld collapse) of the polymers to be joined is the required value for the process output to terminate the welding process. This means that when the targeted meltdown value is reached during laser transmission welding, the process is automatically terminated (laser is turned off). Before welding, the polymer assembly is clamped and the sensor sets

the reference point, from which the meltdown measurements will start during processing. Once the reference point is set, the laser is turned on and welding begins, and the laser transparent and laser absorbent parts melt to form a permanent joint. When the sensor detects that the targeted meltdown has been reached, the laser is turned off. The clamping force works not only during heating, when the laser is turned on, but also during cooling. Joint cooling is applied after the heating phase, when the laser is turned off, and continues until the joint is fully solidified and cooled for a defined period of time. The targeted meltdown is selected based on the geometry and size of the polymer assembly.

Heating time [s], laser power [W], clamping force [N], and meltdown [mm] values were recorded during sample production. The variable parameters of quasi-simultaneous laser welding were laser power, scanning speed, clamping force, and laser beam shift from the centre of the weld seam. The welding process parameters for I-30, II-20, and III-m polymer pairs are shown in Table 3 and they were constant during all tests. Different scanning speeds for the polymer pairs were selected based on the different laser transmissions of the transparent parts.

The welding parameters for determining the range of process parameters and for improving the joint quality of III-m joints are presented in Table 4. The laser power was varied in the range of 330 W to 400 W.

2.3. Study of the weld seam structure

A cross-sectional study was performed to evaluate the formation of welds, defects, and the heat-affected zone (HAZ). Specimens for cross-sectional testing were prepared by cutting sections from the welded polymer pairs using a WELL Diamond Wire Saw 4500, followed by grinding and polishing operations. Cross-sectional images were acquired and examined using a Keyence VHX-6000 digital microscope.

2.4. Burst pressure test

A burst pressure test was performed at room temperature to evaluate the strength of the welded joints. A welded part (polymer pair) with closed geometrical contour was taken, a hole was drilled to connect it to the burst tester and a screw nipple was screwed in. A jet of distilled water at a pressure of 150 mbar (starting from 0 mbar) was used inside the welded parts. Burst pressure was cut off when cracks appeared and the maximum pressure was recorded.

2.5. Thermal shock and leakage tests

To evaluate the tightness of the welds, thermal shock and leakage tests were performed, which are presented in Table 5. The temperatures ranged from –30 °C to +120 °C.

Table 3. Quasi-simultaneous laser welding process parameters

Parameters	Units	Polymer pair (laser transparent/laser absorbent)		
		I-30	II-20	III-m
Laser power	W	360	370	370
Scanning speed	mm/s	1400	1000	1400
Cooling time	s	3.5		
Clamping force	N	2700		
Laser beam diameter	mm	3		

Table 4. Welding process parameters of III-m joints

Parameters	Units	Parameter sets			
		PI	PII	PIII	PIV
Laser power	W	330	340	350	400
Scanning speed	mm/s	1400			
Cooling time	s	3.5			
Clamping force	N	2700	2400	2700	
Laser beam diameter	mm	3			

(a)

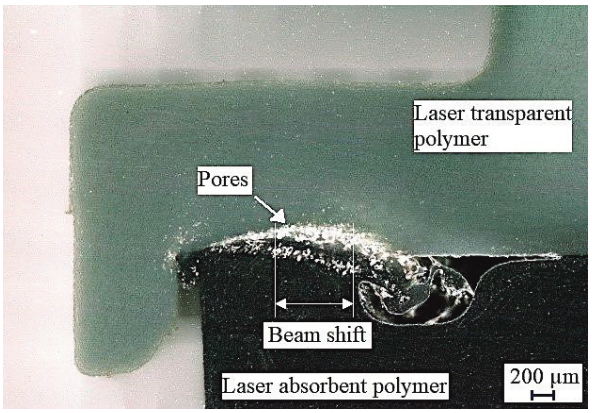

(b)

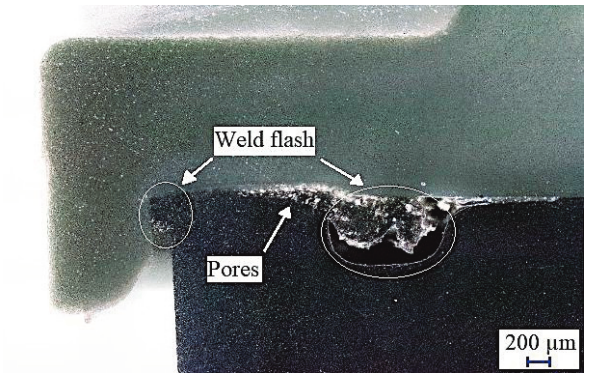

(c)

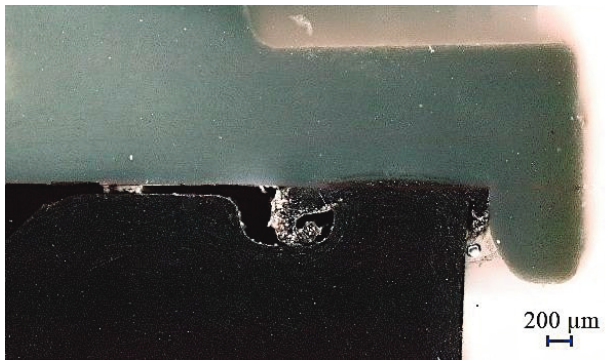

Fig. 4. Cross-sectional images of a weld depicting laser beam shift from the weld: (a) 0.7 mm; (b) 0.4 mm; (c) 0.0 mm.

A similar situation was observed at a slightly different position of the laser beam, at a distance of 0.4 mm from the weld centre, and the cross-sectional view shows fewer pores (Fig. 4b). Stronger welds were achieved at an average burst pressure of 6.2 bar. Compared to previous results, a shorter heating time of up to 4.9 s was required to achieve the targeted meltdown with a 0.4 mm shift. In addition, it is worth noting that the shift of the laser beam from the centre of the weld seam affects the inhomogeneous melting, as can be clearly seen in Fig. 4a and b, where the weld flash is mainly concentrated where the laser beam enters the polymer interface. At the shifts of 0.7 mm and 0.4 mm, the welding flash is more focused on the left side where the laser beam has been shifted (Fig. 4a and b).

Further tests were performed with a shift of 0.0 mm. Laser power, scanning speed, clamping force and cooling time were kept unchanged to compare the welding quality with the previous welding results. At a shift of 0.0 mm, a maximum average bond strength of 6.4 bar was achieved with a minimum heating time of 4.2 s. This can be explained by the homogeneous melting of the polymer throughout the weld during QSLW, which allowed to achieve the targeted meltdown faster than more significant laser beam shifts. Also, the cross-sectional images (Fig. 4c) showed a more homogeneous distribution of the weld flash in both directions inside the polymer joint, indicating that the laser beam enters the centre of the weld and evenly melts the polymer interface.

The results of the joint structure and strength can be further explained by the energy input from the laser radiation during welding. With a longer heating time, more laser beam passes are used to achieve the targeted meltdown of 0.30 mm. The energy input for joint formation increases with the increase in the number of passes [14–16]. More energy is required to achieve the targeted meltdown of 0.30 mm at laser beam shifts of 0.7 mm and 0.4 mm compared to 0.0 mm. Meltdown can only occur if the entire weld interface area melts and if polymer parts are subjected to external clamping forces [17,18]. It can be said that the interface temperature of the PPAGF40 joint increases uniformly when the centre of the laser beam path is aligned with the centre of the weld. The positioning of the laser beam during welding strongly affected the formation of defects and the strength of the joint.

3.2. Effect of position on joint heating time

For a more in-depth analysis of the positioning of the laser beam based on the heating time of PPAGF40, the production monitoring of 460 samples was performed to perform a statistical evaluation of the results. In this study, pairs of II-20 polymers were selected, and their heating times during sample production were recorded and compared. The targeted meltdown of 0.32 mm remained the same for all welded parts. Laser power, scanning speed, cooling time, and clamping force did not change during the QSLW tests. The shift of the laser beam from the joint was modified by creating new laser weld contours as shown in Fig. 5a and b.

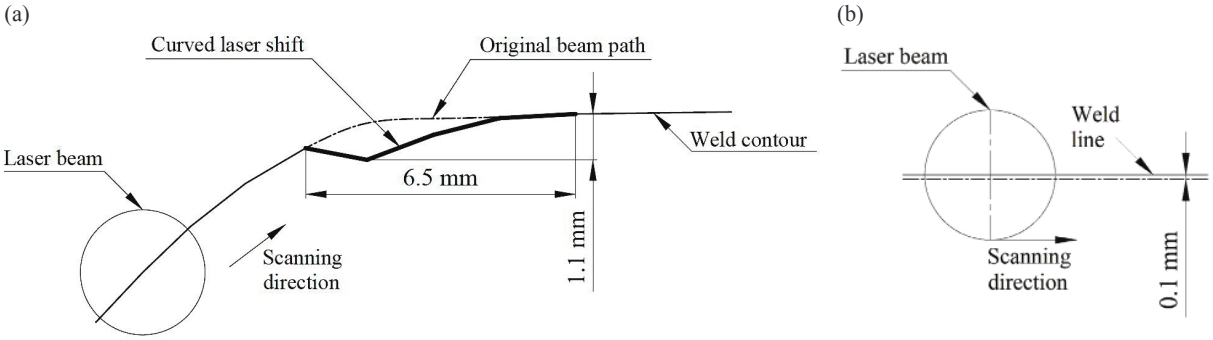

Fig. 5. Schemes of laser irradiation: (a) curved laser beam shift of 6.5 × 1.1 mm, created at the corner of the weld contour; (b) laser beam shift of 0.1 mm.

After creating a new laser beam scanning position on the weld with a curve and shift of 0.1 mm, the next step was to monitor the heating time of PPAGF40 required to achieve the predefined meltdown. The increased heating time observed in Fig. 6 suggests that shifting the laser beam away from the weld affected the inhomogeneous distribution of temperature in the joint and the melting during QSLW.

Figure 6 shows that at a 0.1 mm laser beam shift from the weld centre, a shorter polymer heating time with an average value of 4.6 s is required to achieve the targeted meltdown. In this case, the energy transfer from the laser resulted in a more uniform melting and temperature distribution than the curved laser beam scan path, with an average heating time of 5.3 s. Based on the presented results, it can be stated that the positioning of the laser beam on the weld is a critical setup in the QSLW process, which significantly impacts the weld quality and heating time.

3.3. Effect of position correction and laser power

To gain deeper knowledge about the influence of laser beam positioning on the performance of the polymer joint, thermal shock and weld leakage tests were performed on the produced samples (test conditions are presented in Table 5). This study used III-m pairs with modulated polymer transmission through the transparent part. Initial welding tests of the III-m polymer pairs were performed using the same laser welding scan path with a curved laser beam shift as in the previous study. A targeted meltdown value of 0.30 mm was selected to complete the welding process. The initial parameters of quasi-simultaneous welding were P_L = 370 W, v_s = 1400 mm/s, cooling time 3.5 s and clamping force 2700 N.

Thus, when a curved laser beam shift was previously created from the weld centre, the III-m pairs showed leaky welds after 50 thermal shock cycles in the area where the curved beam path was created. The leakage of the polymer

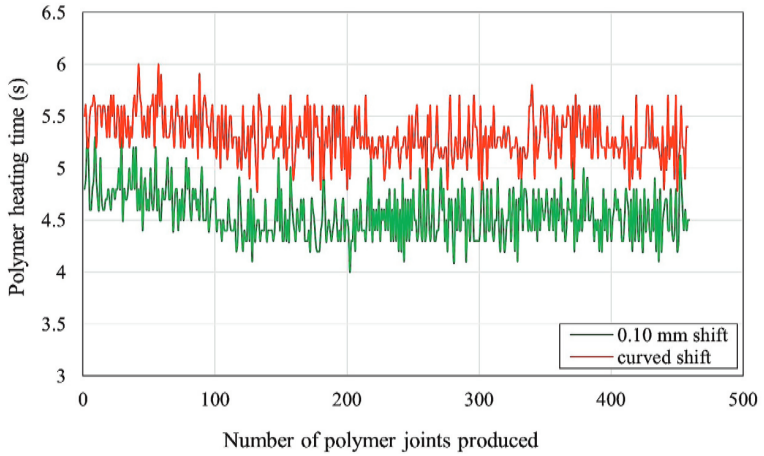

Fig. 6. Heating time of II-20 polymer pairs with different laser beam shifts from the weld.

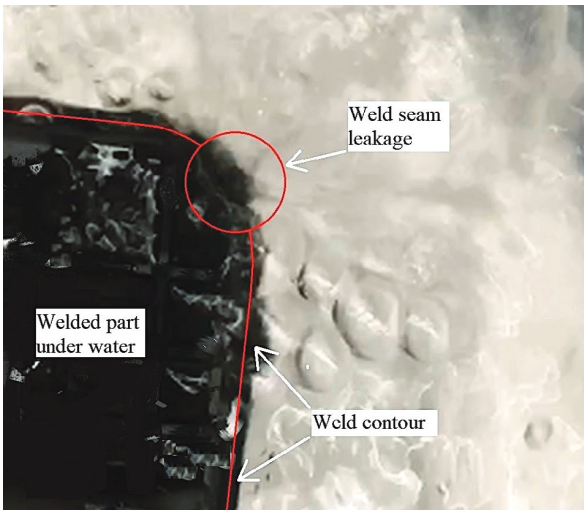

Fig. 7. View of III-m weld seam leakage under water.

joint can be explained by poor melting of welds where the laser beam has a curved scan path. Poor melting and adhesion between the laser transparent and laser absorbent polymer parts contributed to the degradation and cracking after thermal shock, resulting in weld leakages after 50 thermal shock cycles (Fig. 7).

To prevent weld leakage and to avoid degradation of the polymer joints after 50 thermal shock cycles, the weld quality was improved by creating a laser beam positioning with a 0.0 mm shift. Nevertheless, the cross-sectional study revealed that even at a laser beam shift of 0.0 mm from the centre of the weld, the III-m polymer pairs exhibited pore formation inside the joint. Although Fig. 8a and b show a homogeneous squeeze flow of weld flash inside the weld, an observation of the pore distribution shows that the highest concentration of pores was formed in the centre of the weld. This can be explained by the Gaussian intensity distribution of the laser beam within the maximum intensity at the centre of the laser beam. This influenced overheating in the middle of the weld seam in the areas of the III-m joints where the transmission of the transparent part was highest. The HAZ was generated and spread around the perimeter of the joint (Fig. 8a). It is important to note that all samples withstood 50 thermal cycles, showed no weld leakage under water and failed only after the 75th cycle. It is not entirely clear whether having no leakage after 50 thermal cycles was due to the reduced shift of the laser beam from the centre of the joint, given that the modulated laser transmission affects the inhomogeneous energy deposition and the temperature distribution around the weld perimeter during welding. Therefore, there is always a risk and possibility that pores might form inside the joints.

Further research was carried out to create defect-free weld zones and increase the tightness of the polymer joint. Welding tests were performed by changing the laser power and thus the energy input to the weld [14–16]. Since the initial III-m processing parameters caused weld defects, the next step was to reduce the P_L to slow the temperature rise and avoid overheating at the polymer interface, given that the temperature rises during QSLW [4,19]. To adapt the optimal process parameters for the III-m polymer pairs, the laser power was varied from 330 W to 400 W (test conditions are given in Table 4).

First, welding tests with the parameter set PI were performed using P_L of 330 W and a clamping force of 2700 N. The cross-section of the produced welds showed reduction of the HAZ and a poreless weld seam (Fig. 9a) in comparison with the joints produced with P_L of 370 W (Fig. 8). The observed heating time reached up to 6.1 s.

Welding tests with the parameter set PII were performed using P_L of 340 W and a clamping force of 2400 N. Figure 9b shows that reducing the P_L by 30 W from the

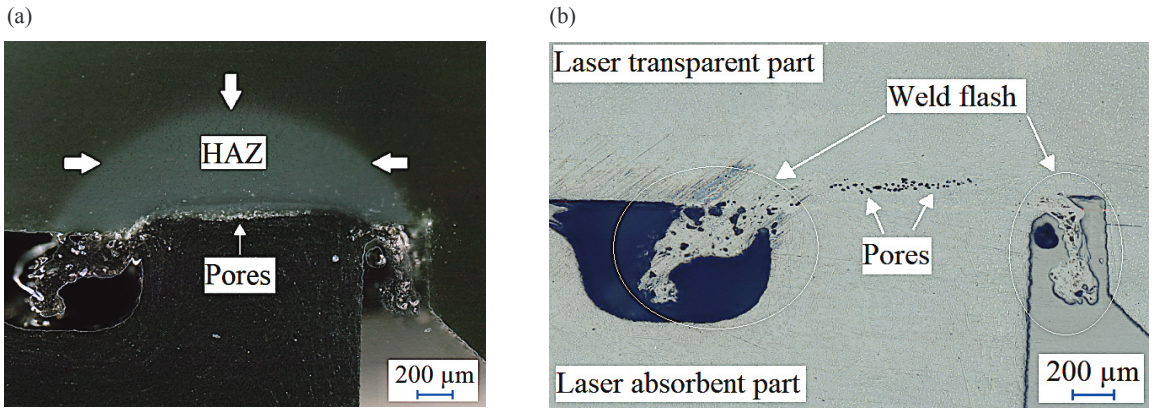

Fig. 8. Cross-section of the III-m weld seam: (a) HAZ and polymer overheating with pore formation; (b) distribution and concentration of pores under different illumination.

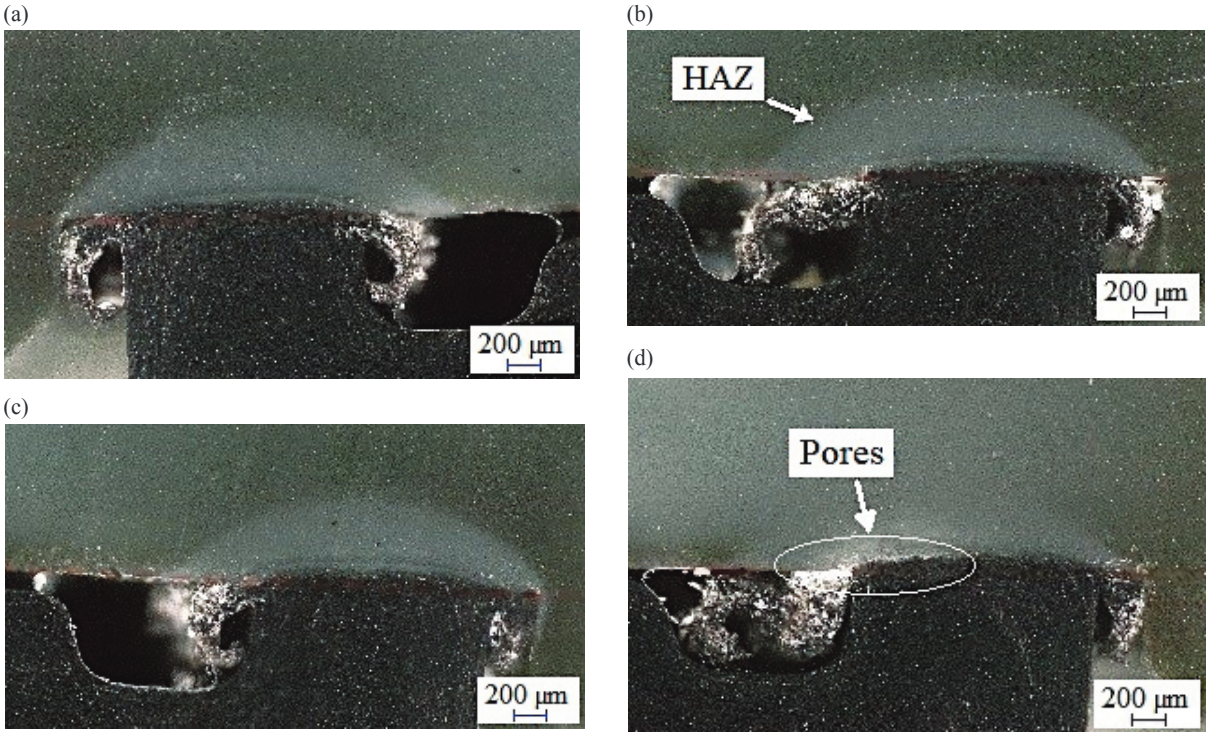

Fig. 9. III-m cross-sections produced with different parameter sets: (a) PI; (b) PII; (c) PIII; (d) PIV.

initial laser power of 370 W significantly reduced the HAZ, and no pore formation was detected in the cross-section. The polymer heating time required to achieve the targeted meltdown for the III-m polymer pair at P_L of 340 W varied from 5 to 5.4 s.

Welding experiments using the parameter set PIII were performed with a 10 W higher laser power of 350 W and a clamping force of 2700 N. Similar results were obtained in the case described above, where no pores or other defects such as cracks or burn marks were detected in the weld (Fig. 9c), and only a slightly reduced heating time was observed during sample formation, with a minimum heating time of 4.7 s. A targeted meltdown can be achieved faster with higher laser power [20].

Finally, P_L was increased to 400 W (parameter set PIV) to obtain laser welding process parameters for III-m polymer pairs. As expected, P_L of 400 W resulted in excessive energy input and rapid heating of the polymer interface, forming pores inside the weld (Fig. 9d).

When the optimal parameters of the laser welding process had been determined, a leakage test was performed on III-m joints after 50, 75 and 100 thermal shock cycles. Thus, in order to evaluate the tightness of the polymer weld zone and to compare it with previous results, the same test conditions were implemented: pressure flow of 300 mbar to the welds under water, test duration of 7 s to see the formation of bubbles. After 50, 75 and 100 temperature shock cycles, no leakage of the weld zone was detected. The increase in the tightness of the weld is due to homogeneous melting achieved by a 0.0 mm laser beam shift from the weld with the help of PL adjustment. No external or internal joint defects were detected.

A burst pressure test was performed on the III-m joints to determine the weld strength experimentally. All samples withstood the burst pressure of more than 5 bar in the P_L range of 330 W to 350 W. The burst pressure of the parts produced using P_L of 400 W was also evaluated, which allowed a more accurate determination of the parameter range of the quasi-simultaneous welding process. The strength results obtained by P_L of 400 W showed the reduction of burst pressure by less than 5 bar on average, which is caused by the formation of pores inside the polymer joint [21]. The results of joint strength are shown in Fig. 10.

Improvement of the QSLW process for the III-m polymer pairs using a 0.0 mm laser beam shift and P_L adjustments showed advantages in joint formation and performance. It should be emphasized that the positioning of the laser beam on the weld and the laser power are critical parameters for QSLW processing. Decreasing the

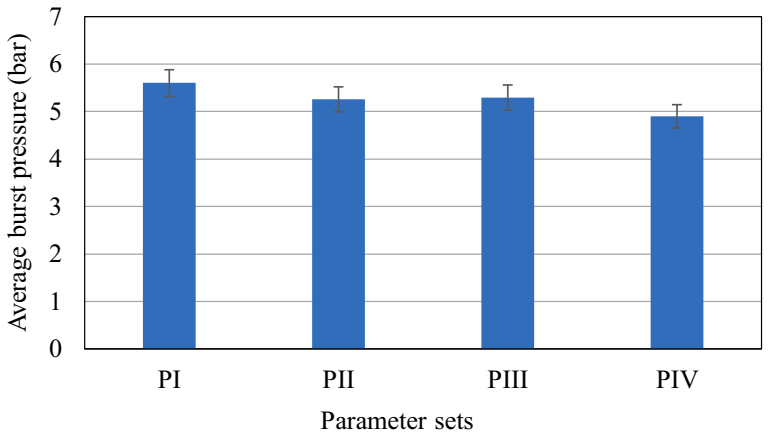

Fig. 10. Strength of a III-m polymer pair produced by different parameter sets.

laser power reduced the size of the HAZ and the number of defects in the polymer bond.

4. CONCLUSIONS

The positioning of the laser beam directly impacts the formation of polymer weld defects, the heating time required to achieve the targeted meltdown, and the weld strength.

1. No defects were detected in the polymer pairs with uniform laser transmissions of 20% and 30% through the transparent part when the laser beam shift from the joint centre was 0.0 mm, which ensured homogeneous melting of the polymers. Modulated laser transmission in the range of 27% to 47% induced inhomogeneous energy deposition along the joint perimeter, resulting in the formation of heat-affected zones and pores.
2. The shift of the laser beam from the centre of the weld increased the heating time required to achieve the targeted meltdown, caused by non-uniform melting and energy distribution in the weld. The shortest heating time is obtained for polymer pairs using a 0.0 mm shift with uniform and modulated laser transmission through the transparent part.
3. The strongest welds were obtained by positioning the laser beam on the weld seam with a shift of 0.0 mm for polymer pairs with uniform laser transmission. The cross-sectional examination did not show any defects in the weld.
4. The quality of the polymer joint with modulated laser transmission through the transparent part is improved using a 0.0 mm laser beam shift in the weld together with laser power adjustment.

ACKNOWLEDGEMENT

The publication costs of this article were partially covered by the Estonian Academy of Sciences.

REFERENCES

1. Potente, H., Wilke, L., Ridder, H., Mahnken, R. and Shaban, A. Simulation of the residual stresses in the contour laser welding of thermoplastics. *Polym. Eng. Sci.*, 2008, **48**(4), 767–773. https://doi.org/10.1002/pen.20999
2. Gonçalves, L. F. F. F., Duarte, F. M., Martins, C. I. and Paiva, M. C. Laser welding of thermoplastics: an overview on lasers, materials, processes and quality. *Infrared Phys. Technol.*, 2021, **119**, 103931. https://doi.org/10.1016/j.infrared.2021.103931
3. Acherjee, B. State-of-art review of laser irradiation strategies applied to laser transmission welding of polymers. *Opt. Laser Technol.*, 2021, **137**, 106737. https://doi.org/10.1016/j.optlastec.2020.106737
4. Acherjee, B. Laser transmission welding of polymers – a review on welding parameters, quality attributes, process monitoring, and applications. *J. Manuf. Process*, 2021, **64**, 421–443. https://doi.org/10.1016/j.jmapro.2021.01.022
5. Bonefeld, D., Schöppner, V., Potente, H., Mahnken, R. and Shaban, A. Residual stresses in the quasi-simultaneous laser transmission welding of amorphous thermoplastics. *Polym. Eng. Sci.*, 2010, **50**(8), 1520–1526. https://doi.org/10.1002/pen.21685
6. Kumar, D., Shekhar Sarkar, N., Acherjee, B. and Kuar, A. S. Beam wobbling effects on laser transmission welding of dissimilar polymers: experiments, modeling, and process optimization. *Opt. Laser Technol.*, 2022, **146**, 107603. https://doi.org/10.1016/j.optlastec.2021.107603
7. Laakso, P., Ruotsalainen, S., Otto, G., Olowinsky, A. and Kujanpää, V. Butt welding of transparent polyamide (PA11)

with 1.94μm fiber laser. *ICALEO*, 2013, **175**. https://doi.org/10.2351/1.5062870
8. Ruotsalainen, S., Laakso, P., Manninen, M., Purtonen, T., Kujanpää, V. and Salminen, A. TWINQUASI – A new method for quasi-simultaneous laser welding of polymers. *ICALEO,* 2012, 262–269. https://doi.org/10.2351/1.5062454
9. Ruotsalainen, S., Laakso, P. and Kujanpää, V. Laser welding of transparent polymers by using quasi-simultaneous beam off-setting scanning technique. *Phys. Procedia.*, 2015, **78**, 272–284. https://doi.org/10.1016/j.phpro.2015.11.038
10. Brodhun, J., Blass, D. and Dilger, K. Laser transmission welding of thermoplastic fasteners: influence of temperature distribution in a scanning based process. *Procedia CIRP,* 2018, **74**, 533–537. https://doi.org/10.1016/j.procir.2018.08.123
11. Wippo, V., Jaeschke, P., Brueggmann, M., Suttmann, O. and Overmeyer, L. Advanced laser transmission welding strategies for fibre reinforced thermoplastics. *Phys. Procedia*, 2014, **56**, 1191–1197. https://doi.org/10.1016/j.phpro.2014.08.034
12. Schkutow, A., Scholle, K., Fuhrberg, P. and Frick, T. Scanning techniques for optimized damage tolerance in quasi-simultaneous laser transmission welding of plastics. *Procedia CIRP*, 2020, **94**, 697–701. https://doi.org/10.1016/j.procir.2020.09.120
13. Nguyen, N.-P., Behrens, S., Brosda, M., Olowinsky, A. and Gillner, A. Laser transmission welding of absorber-free semi-crystalline polypropylene by using a quasi-simultaneous irradiation strategy. *Weld. World*, 2020, **64**, 1227–1235. https://doi.org/10.1007/s40194-020-00913-3
14. Lakemeyer, P. and Schöppner, V. Laser transmission welding of automotive headlamps without a clamping tool. *Weld. World*, 2017, **61**, 589–602. https://doi.org/10.1007/s40194-017-0440-2
15. Ghasemi, H., Zhang, Y., Bates, P. J., Zak, G. and DuQuesnay, D. L. Effect of processing parameters on meltdown in quasi-simultaneous laser transmission welding. *Opt. Laser Technol.*, 2018, **107**, 244–252. https://doi.org/10.1016/j.optlastec.2018.05.047
16. Nguyen, N.-P., Behrens, S., Brosda, M., Olowinsky, A. and Gillner, A. Modelling and thermal simulation of absorber-free quasi-simultaneous laser welding of transparent plastics. *Weld. World*, 2020, **64**, 1939–1946. https://doi.org/10.1007/s40194-020-00973-5
17. Acherjee, B., Kuar, A. S., Mitra, S. and Misra, D. Application of grey-based Taguchi method for simultaneous optimization of multiple quality characteristics in laser transmission welding process of thermoplastics. *Int. J. Adv. Manuf. Technol.*, 2011, **56**, 995–1006. https://doi.org/10.1007/s00170-011-3224-7
18. Lakemeyer, P., Schoeppner, V., Bates, P., Zazoum, B., Zak, G. and DuQuesnay, D. Matching of laser intensity distribution for laser transmission welding of thermoplastics. *Weld. World*, 2017, **61**, 1247–1252. https://doi.org/10.1007/s40194-017-0501-6
19. Wilke, L., Potente, H. and Schnieders, J. Simulation of quasi-simultaneous and simultaneous laser welding. *Weld. World*, 2008, **52**, 56–66. https://doi.org/10.1007/BF03266617
20. Potente, H., Schöppner, V., Bonefeld, D., Wilke, L. and Hage, C. Experiments regarding the influence of pressure profiling on laser-transmission welding. *Weld. World*, 2009, **53**, R246–R252. https://doi.org/10.1007/BF03321136
21. Jankus, S. M. and Bendikiene, R. Effect of the meltdown on thermoplastic joint produced by quasi-simultaneous laser transmission welding. *CIRP J. Manuf. Sci. Technol.*, 2022, **39**, 104–114. https://doi.org/10.1016/j.cirpj.2022.08.001

Laseri positsioneerimine erineva läbipaistvusega polümeeride ülikiirel kontuurlaserkeevitamisel

Simonas Mindaugas Jankus ja Regita Bendikienė

Teadustöö peamine eesmärk oli uurida laserkiire asendi mõju kokkukeevitatavate polümeermaterjalide keevisõmbluse kvaliteedile. Uuringus muudeti laseri kiire liikumise trajektoori esmase keevisõmbluse keskjoone suhtes ja hinnati selle mõju liite vastupidavusele. Analüüsiti kolme läbipaistmatu ja erineva läbipaistvusega polümeeride kombinatsioone, rakendades lõhkesurve-, termolöögi- ja lekkekatseid. Uuringu eesmärk oli hinnata keevisõmbluste tugevust ja hermeetilisust. Suurima tugevusega liide, mille keskmine lõhkesurve oli 6,4 baari, saadi laserkiire liikumisel täpselt keevisjoone keskel ning madalama survetaluvusega liite tugevust 5,8 baari täheldati laserkiire asendi nihkumisel 0,7 mm keevisõmbluse keskjoone suhtes.

Laserkiire trajektoori nihutamine keevisõmbluse keskjoonest eemale põhjustas polümeeride heterogeenset sulamist, mis suurendab etteantud läbisulatuse saavutamiseks vajalikku aega: 4,2 sekundist, kui laserkiir oli täpselt keskjoonel, kuni 10 sekundini 0,7 mm nihke korral. Ebatäpsus toob kaasa liite ülekuumenemise, pooride moodustumise ning seetõttu keevisõmbluse tugevuse vähenemise.

Ülikiirel kontuurlaserkeevitamisel märgati ebaühtlase läbipaistvusega polümeeri ja läbipaistmatu polümeeri kombinatsiooni puhul ebaühtlast energia neeldumist piki keevisliite kontuuri ning termomõjutsooni (TMT) kujunemist. Nende kokkukeevitatud polümeermaterjalide keevisliite kvaliteeti tõsteti, loobudes laserkiire asendi nihutamisest ja rakendades laseri suuremat 300–350 W võimsust. Selle muudatuse tulemusena ei tuvastatud keevisliites leket ka pärast 50, 75 ega ka 100 termilist tsüklit.